SUPPORTING INFORMATION

Manuscript title: **Synthesis and conformational studies of chiral macrocyclic [1.1.1]metacyclophanes containing benzofuran rings**

Author(s): Md. Monarul Islam,[a] Tomiyasu Hirotsugu,[a] Taisuke Matsumoto,[b] Junji Tanaka,[b] Shofiur Rahman,[c] Paris E. Georghiou,[c] Carl Redshaw[d] and Takehiko Yamato*[a]

[a] *Department of Applied Chemistry, Faculty of Science and Engineering, Saga University, Honjo–machi 1, Saga 840–8502 Japan, E–mail: yamatot@cc.saga–u.ac.jp*
[b] *Institute of Material Chemistry and Engineering, Kyushu University, 6-1, Kasugakoen, Kasuga 816-8580, Japan*
[c] *Department of Chemistry, Memorial University of Newfoundland,St. John's, Newfoundland and Labrador A1B 3X7, Canada*
[d] *Department of Chemistry, The University of Hull, Cottingham Road, Hull, Yorkshire, HU6 7RX, UK*

Table of Contents

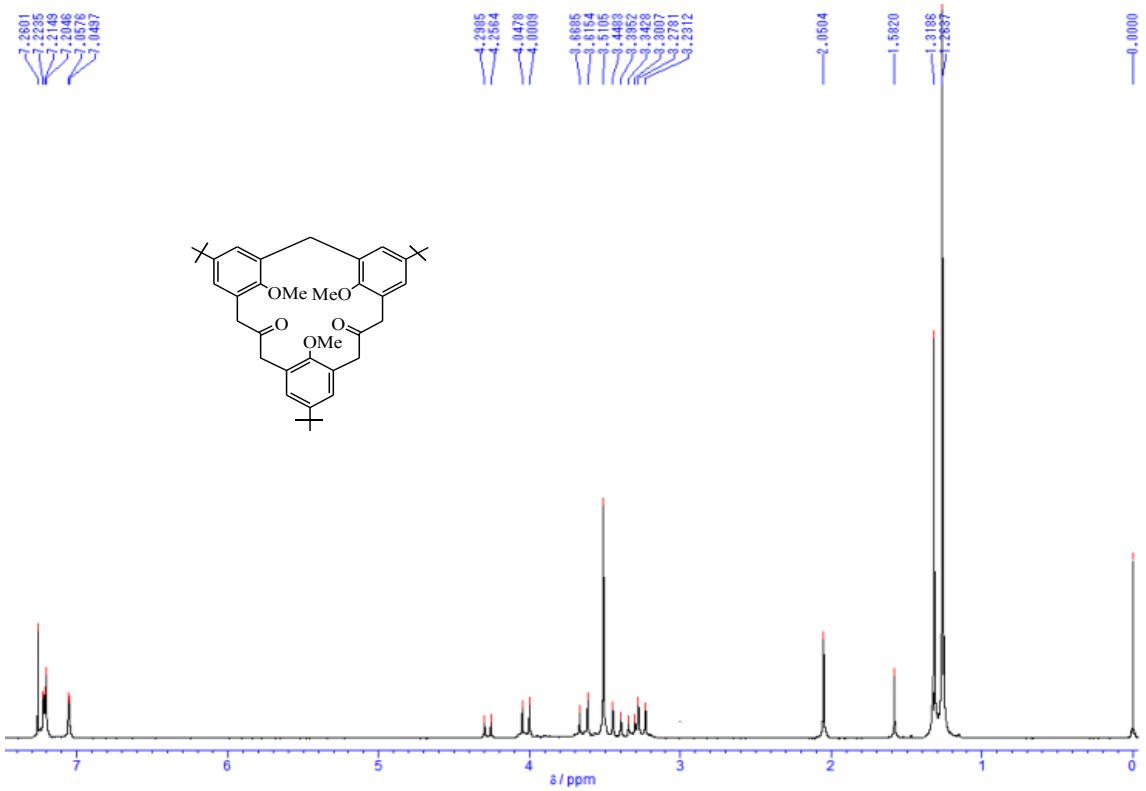

Figure S1: ^{1}H-NMR spectrum (300 MHz, 298 K, $CDCl_3$) of the compound **3**.

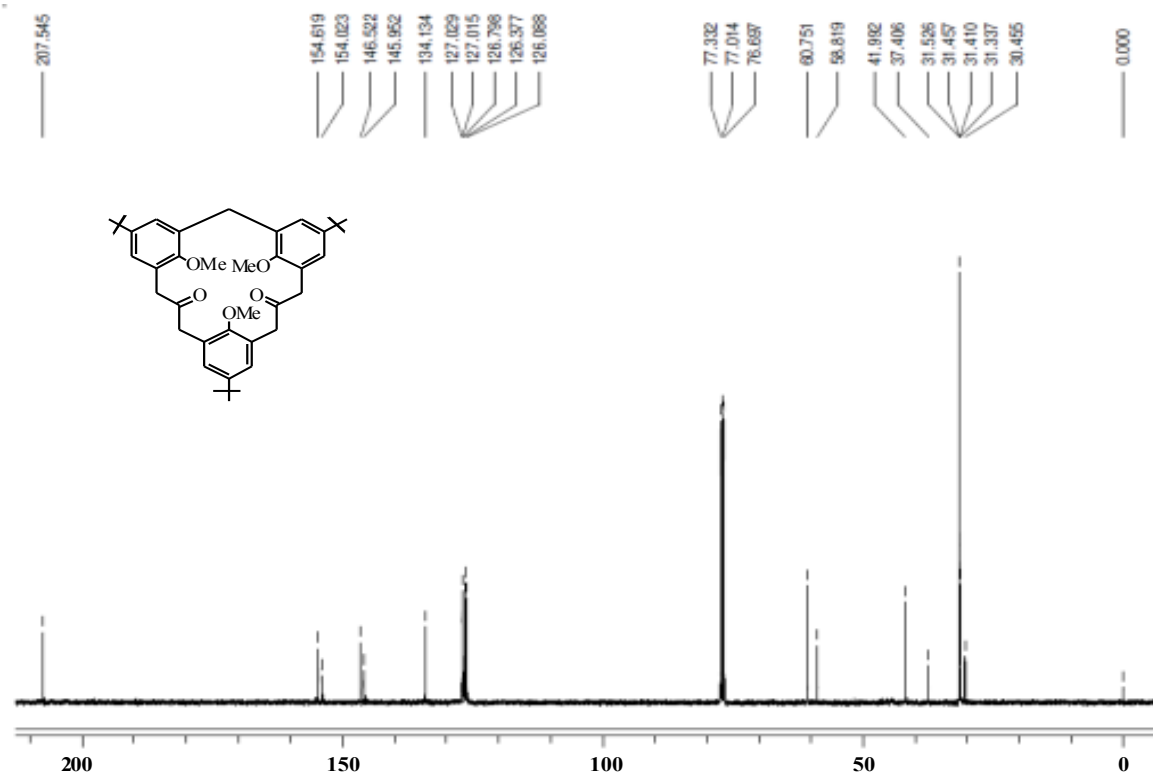

Figure S2: ^{13}C-NMR spectrum (100 MHz, 298 K, $CDCl_3$) of the compound **3**.

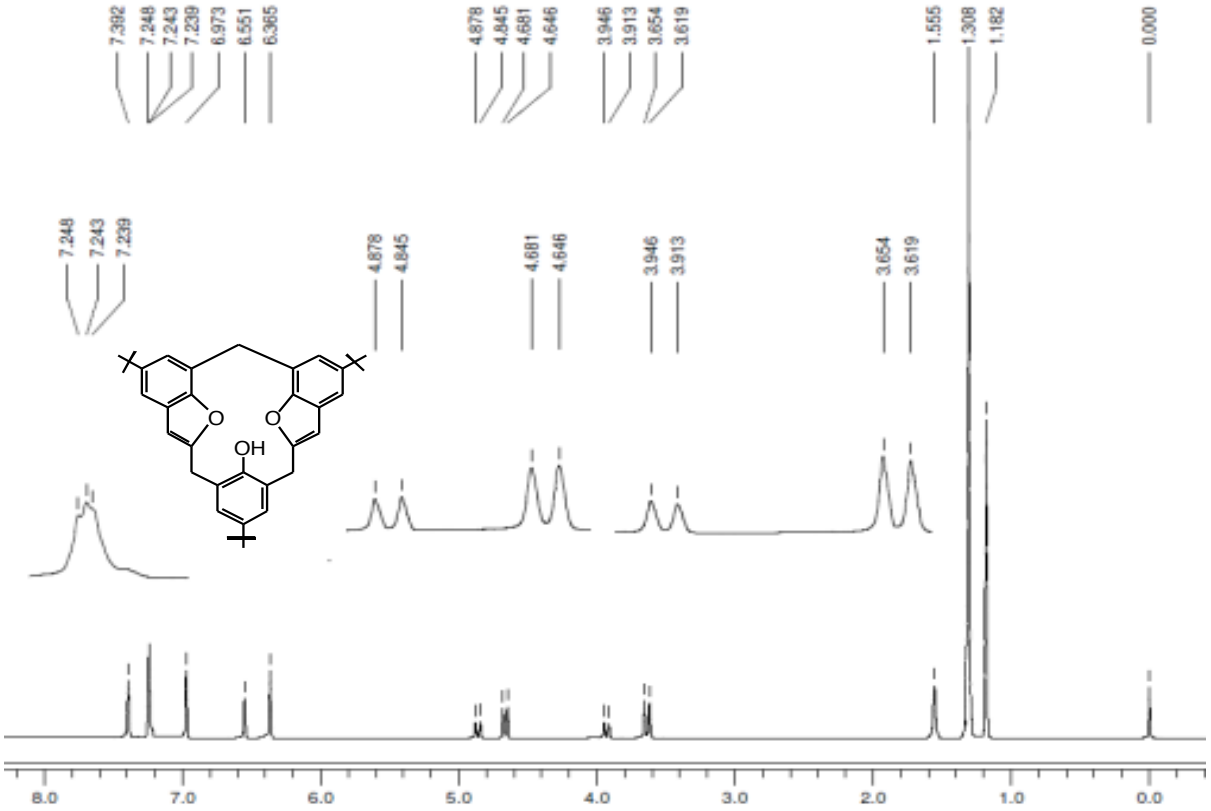

Figure S3: ^{1}H-NMR spectrum (400 MHz, 298 K, $CDCl_3$) of the compound **4a**.

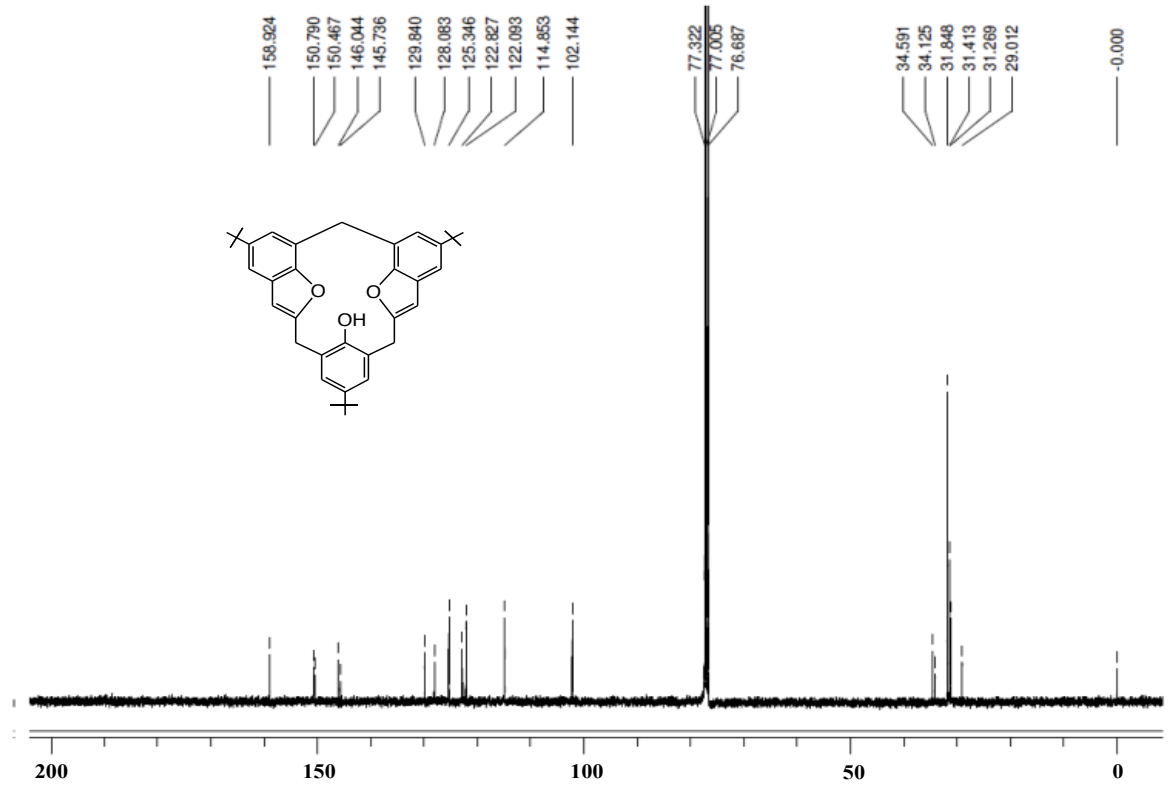

Figure S4: ^{13}C-NMR spectrum (100 MHz, 298 K, $CDCl_3$) of the compound **4a**.

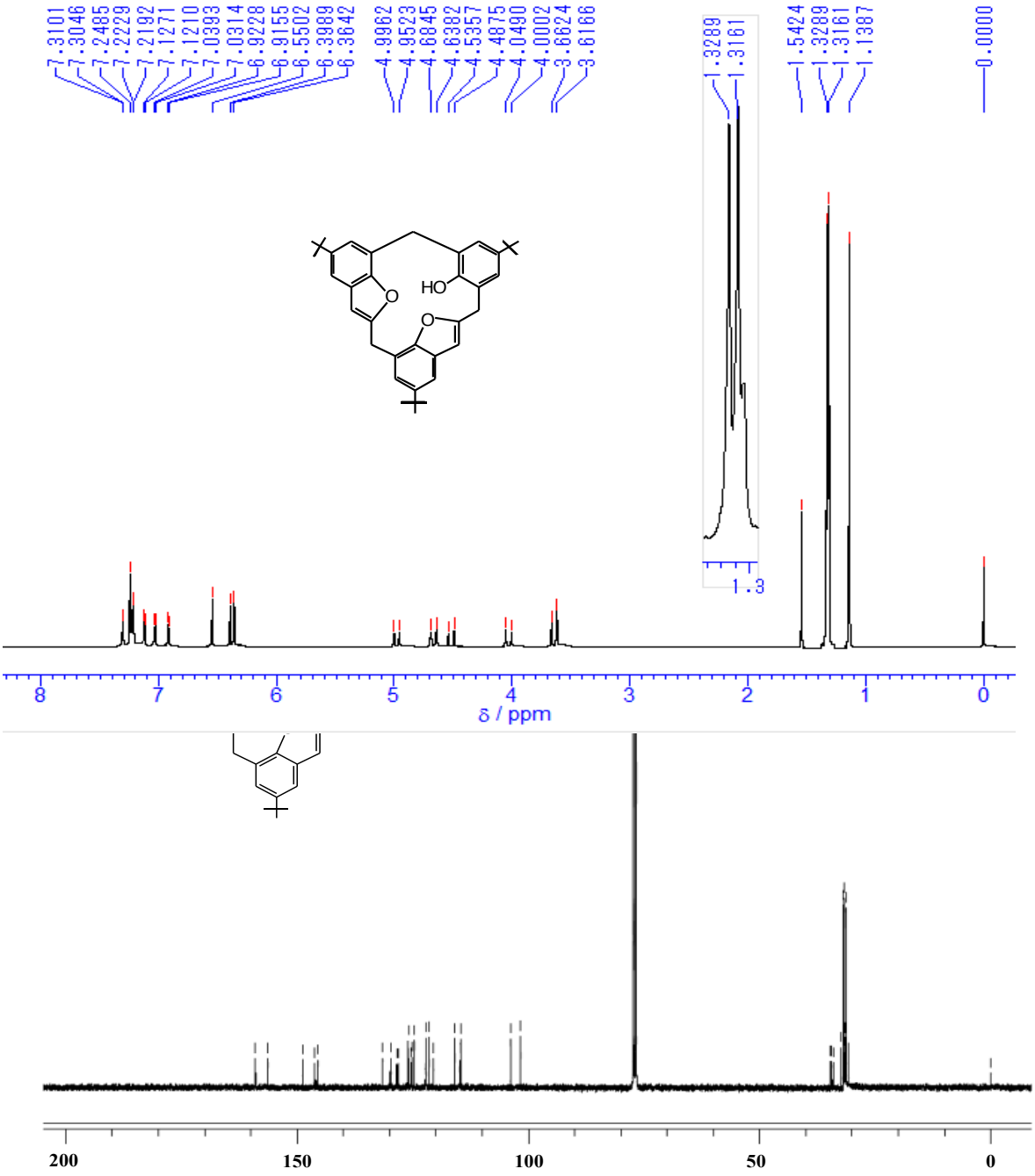

Figure S6: ^{13}C-NMR spectrum (100 MHz, 298 K, $CDCl_3$) of the compound **4b**.

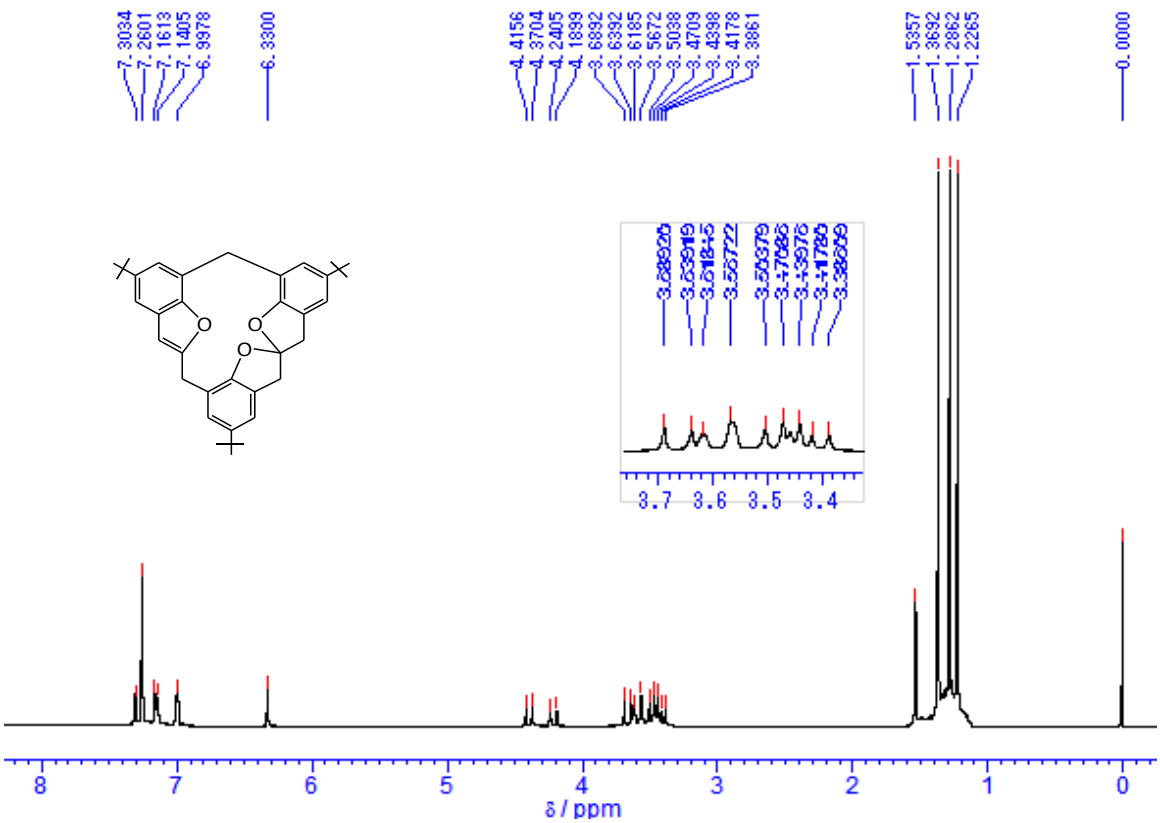

Figure S7: ^{1}H-NMR spectrum (300 MHz, 298 K, $CDCl_3$) of the compound **4c**.

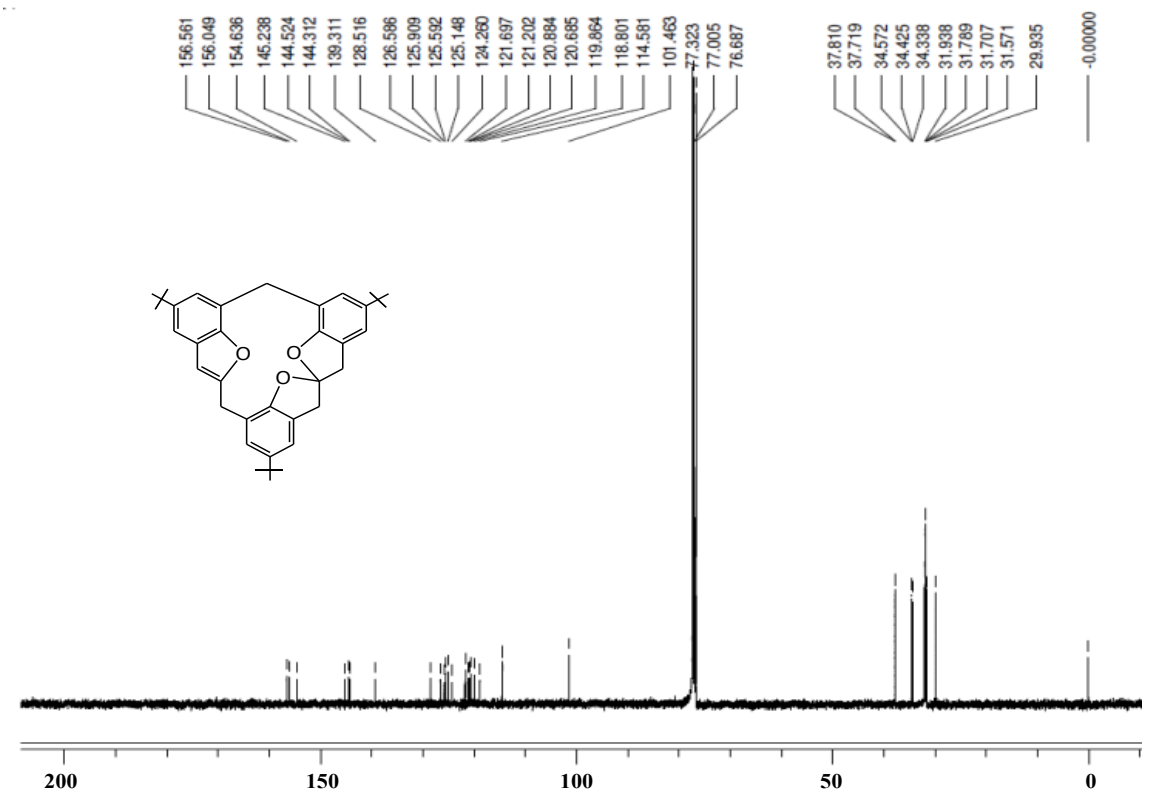

Figure S8: ^{13}C-NMR spectrum (100 MHz, 298 K, $CDCl_3$) of the compound **4c**.

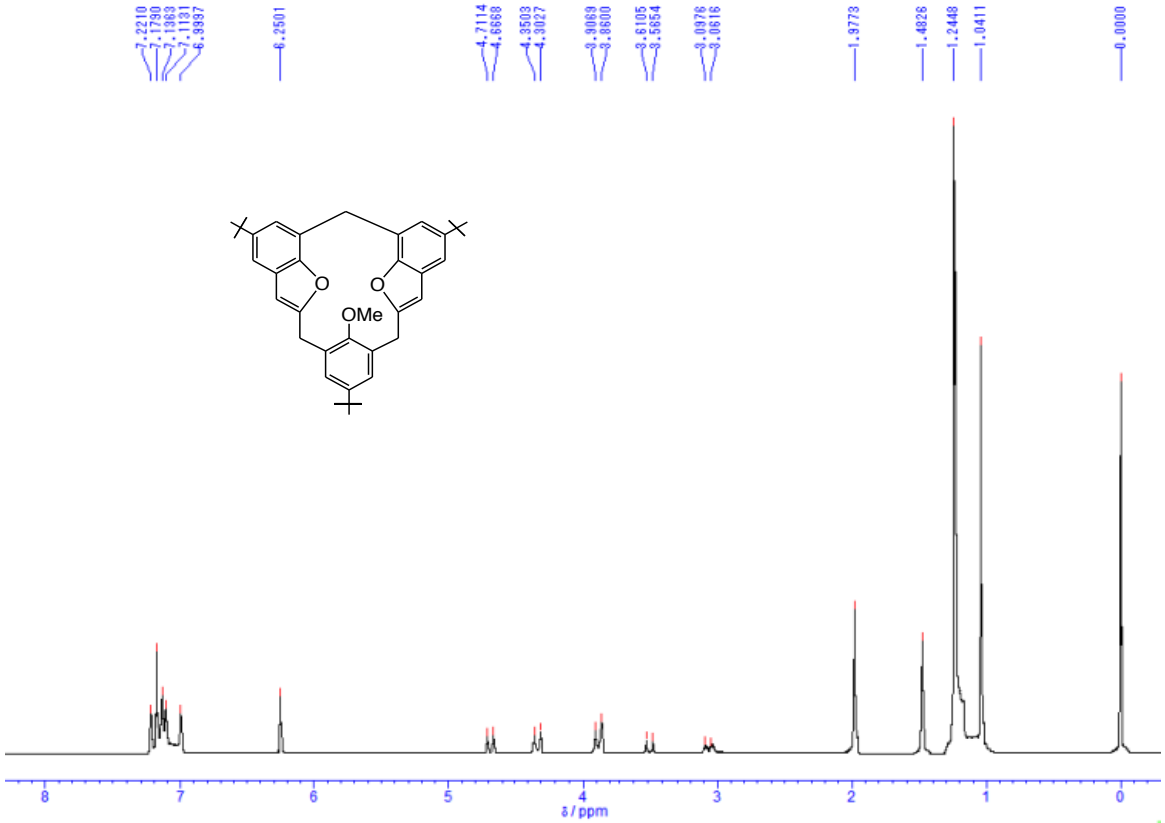

Figure S9: ^{1}H-NMR spectrum (300 MHz, 298 K, $CDCl_3$) of the compound **5a**.

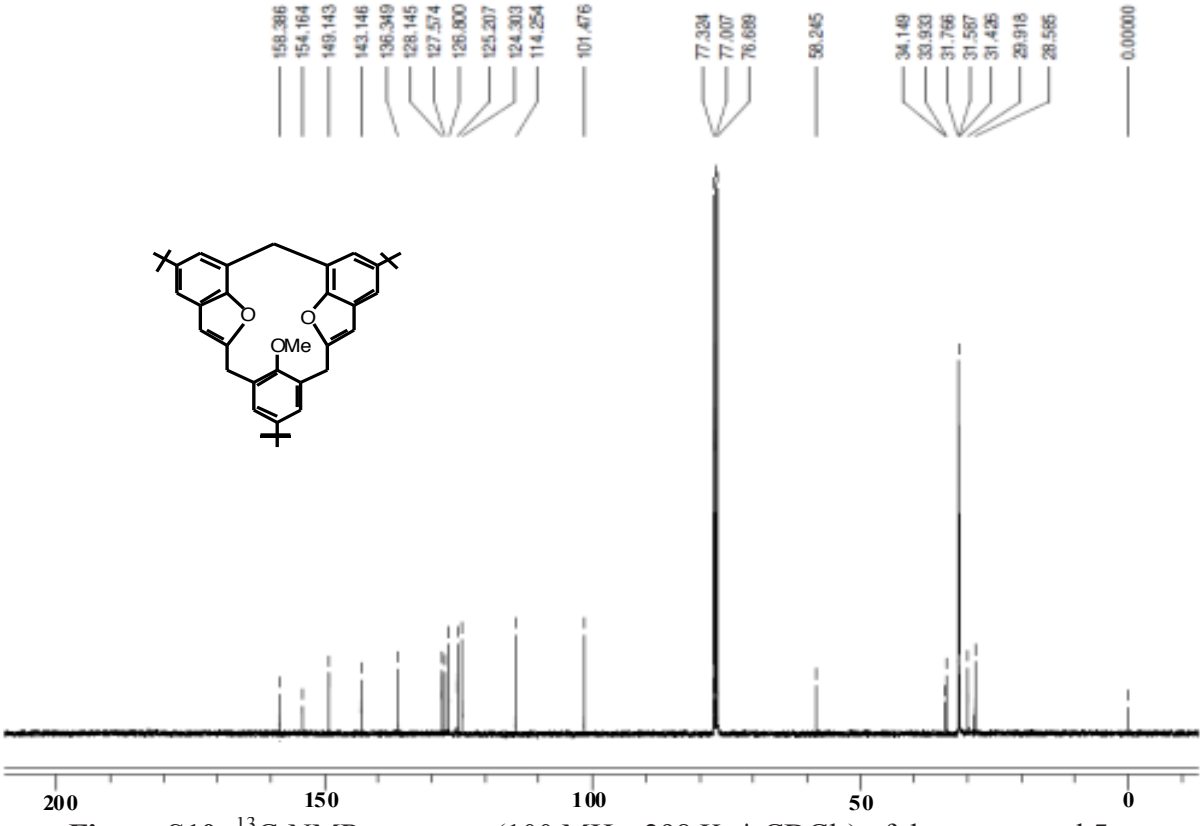

Figure S10: ^{13}C-NMR spectrum (100 MHz, 298 K, * $CDCl_3$) of the compound **5a**.

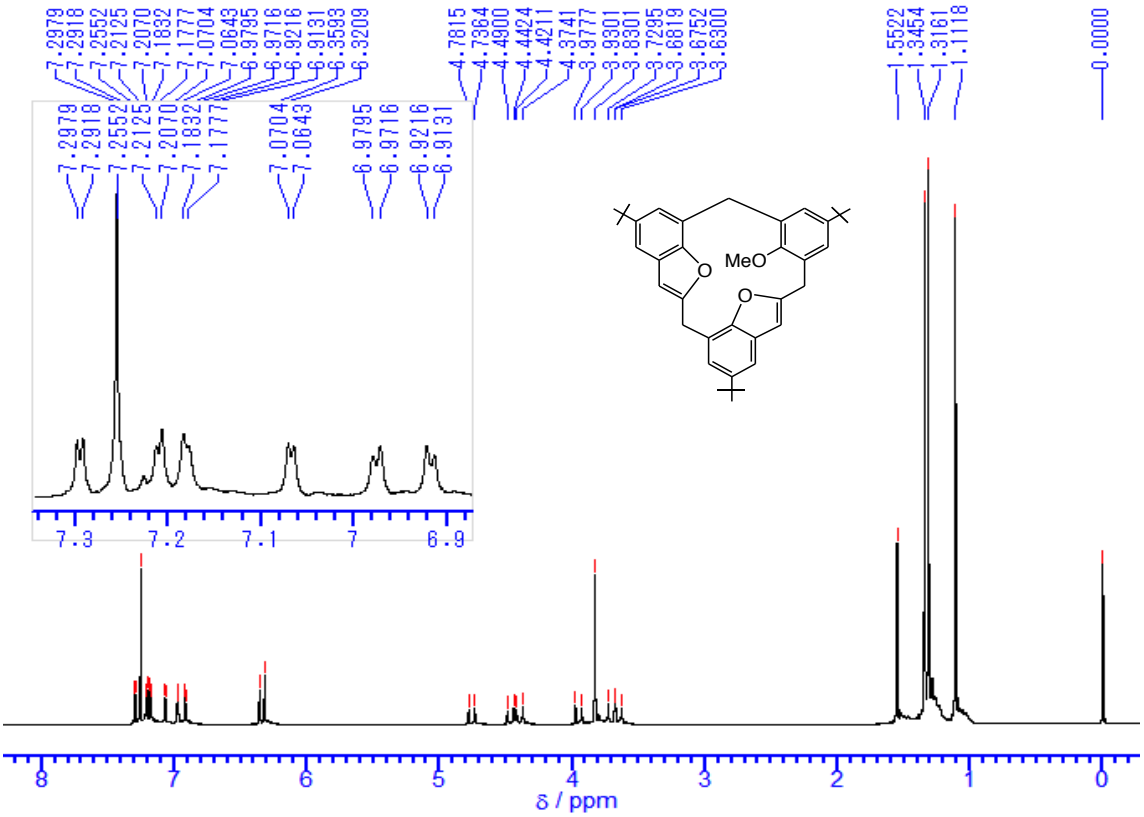

Figure S11: ^{1}H-NMR spectrum (300 MHz, 298 K, $CDCl_3$) of the compound **5b**.

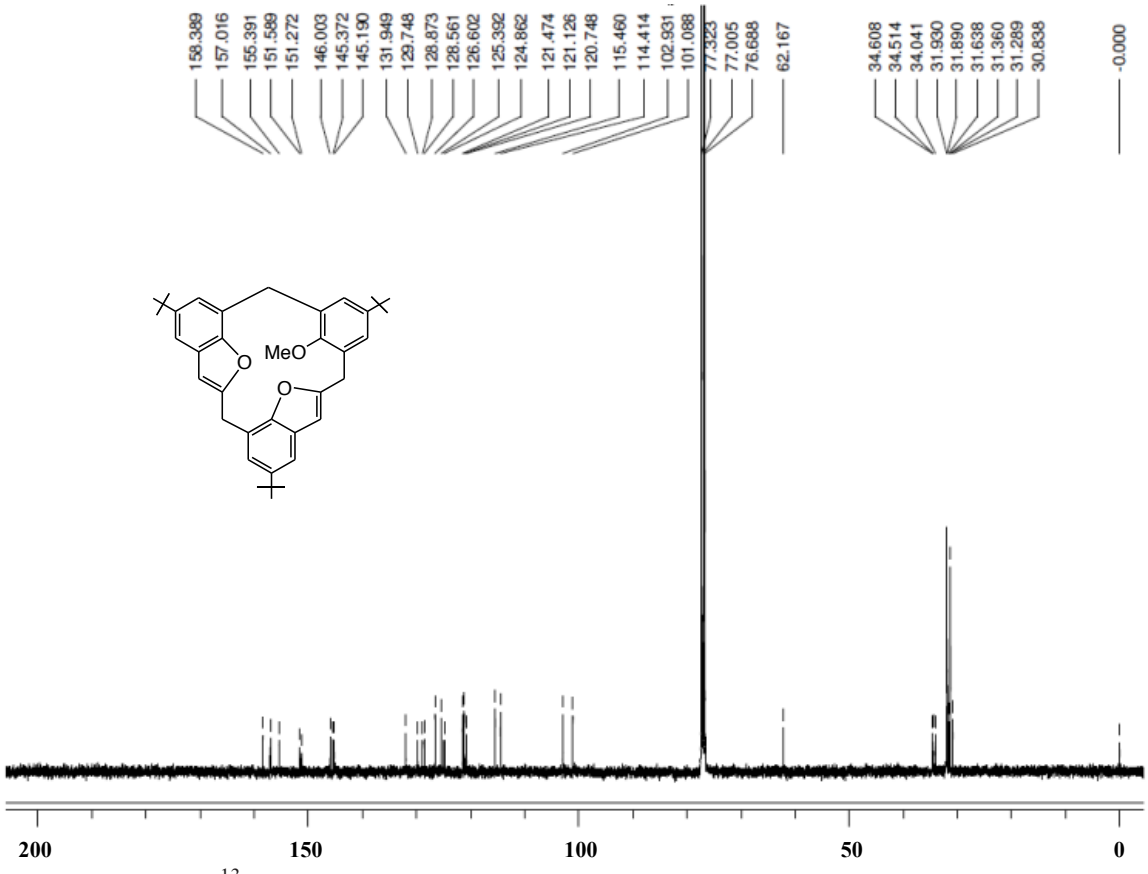

Figure S12: ^{13}C-NMR spectrum (100 MHz, 298 K, $CDCl_3$) of the compound **5b**.

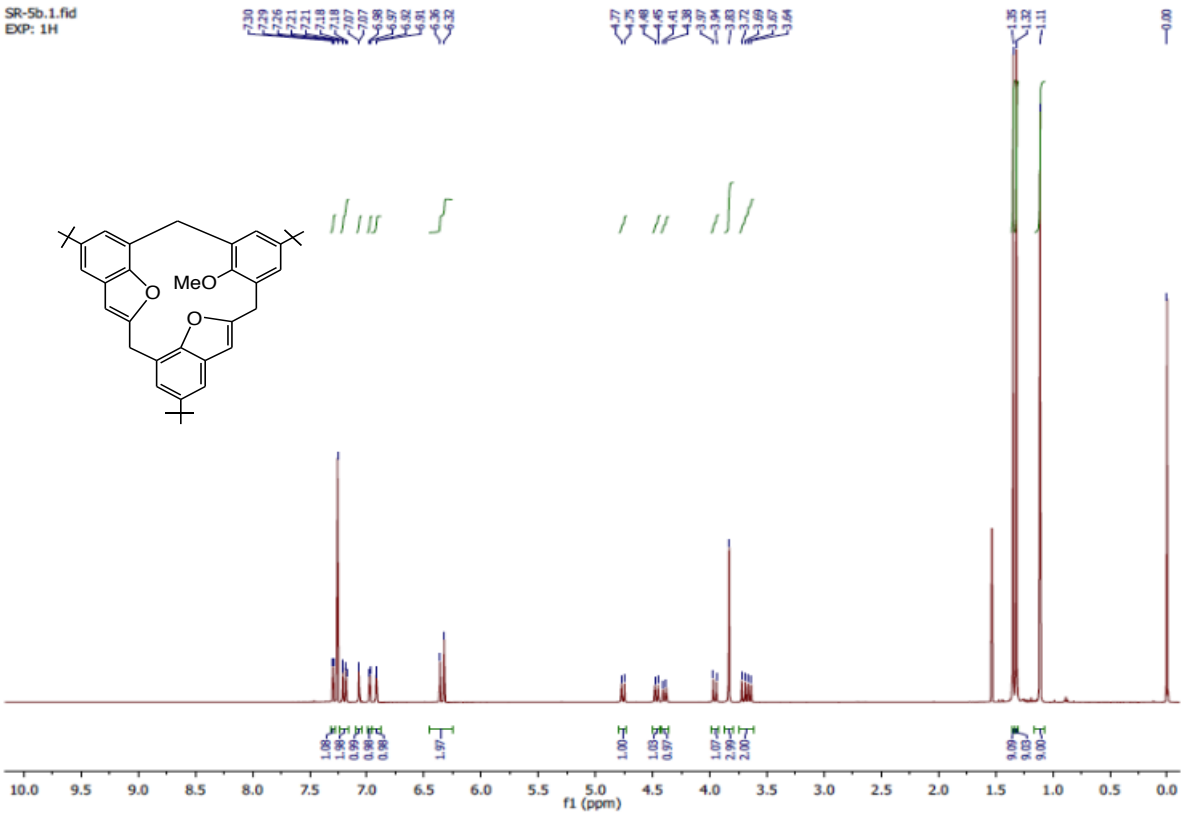

Figure S13: ^{1}H NMR spectra ($CDCl_3$; 500 MHz) **5b**.

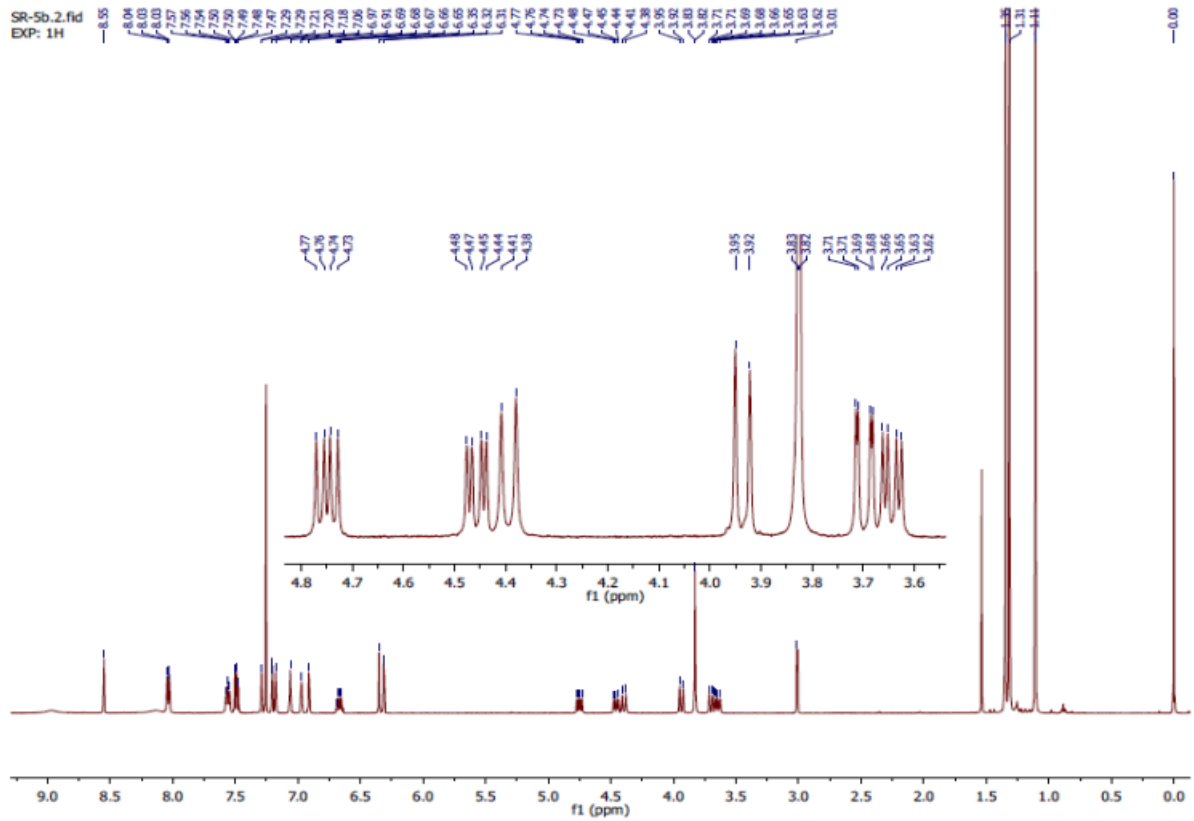

Figure S14: ^{1}H NMR spectra ($CDCl_3$; 500 MHz) **5b** + Pirkle's reagent.

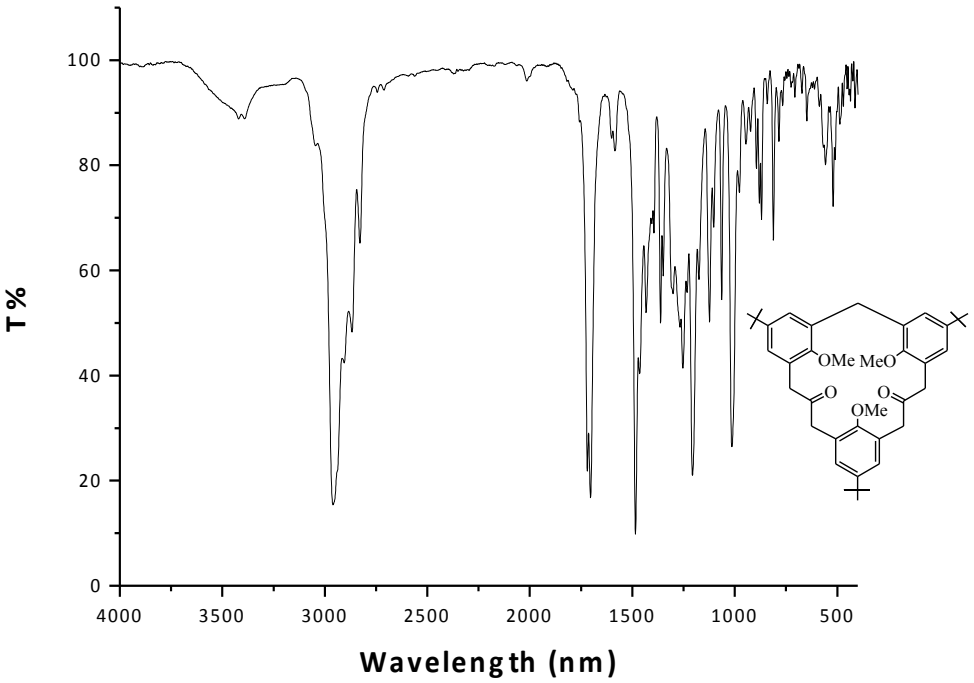

Figure S15: FT-IR spectrum of the compound **3**.

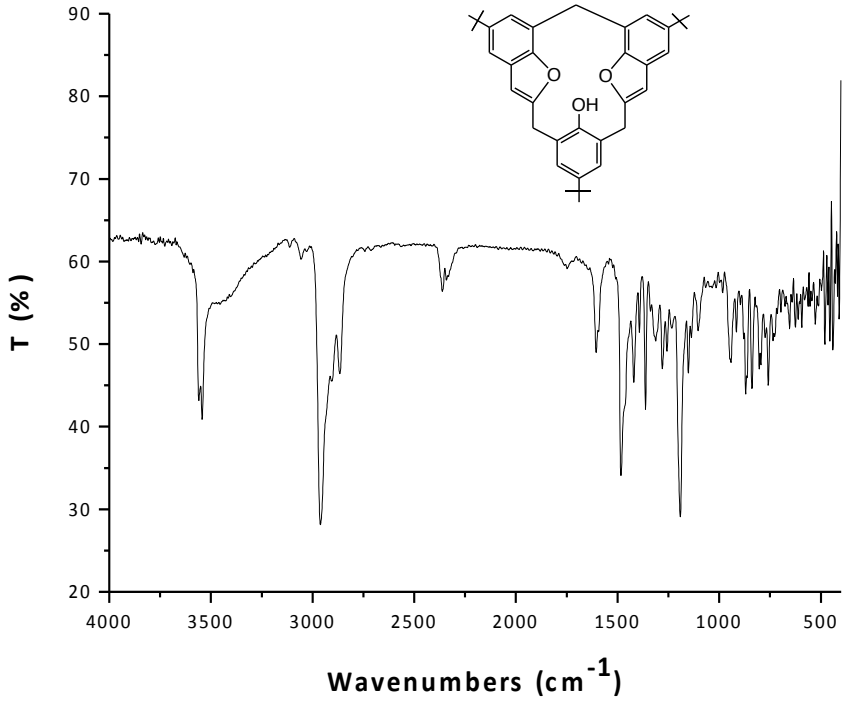

Figure S16: FT-IR spectrum of the compound **4a**.

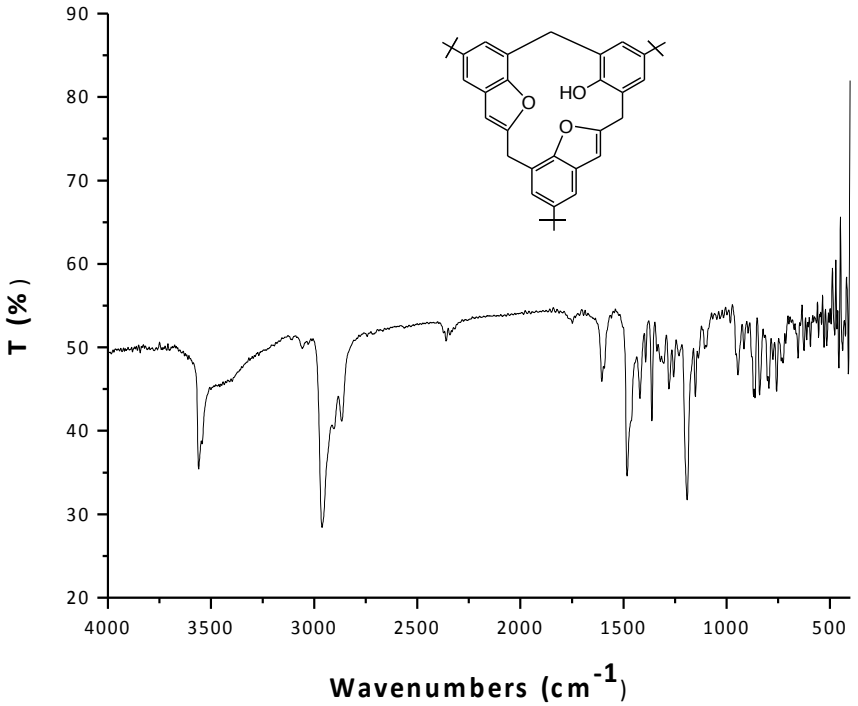

Figure S17: FT-IR spectrum of the compound **4b**.

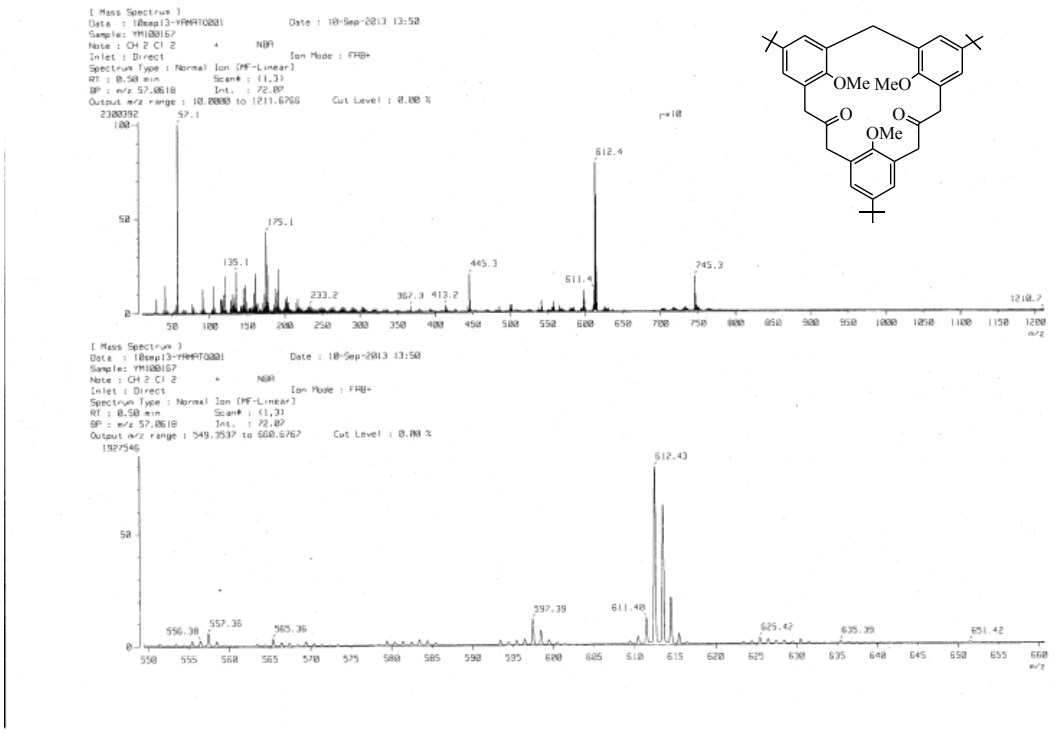

Figure S18: Mass spectrum of the compound **3**.

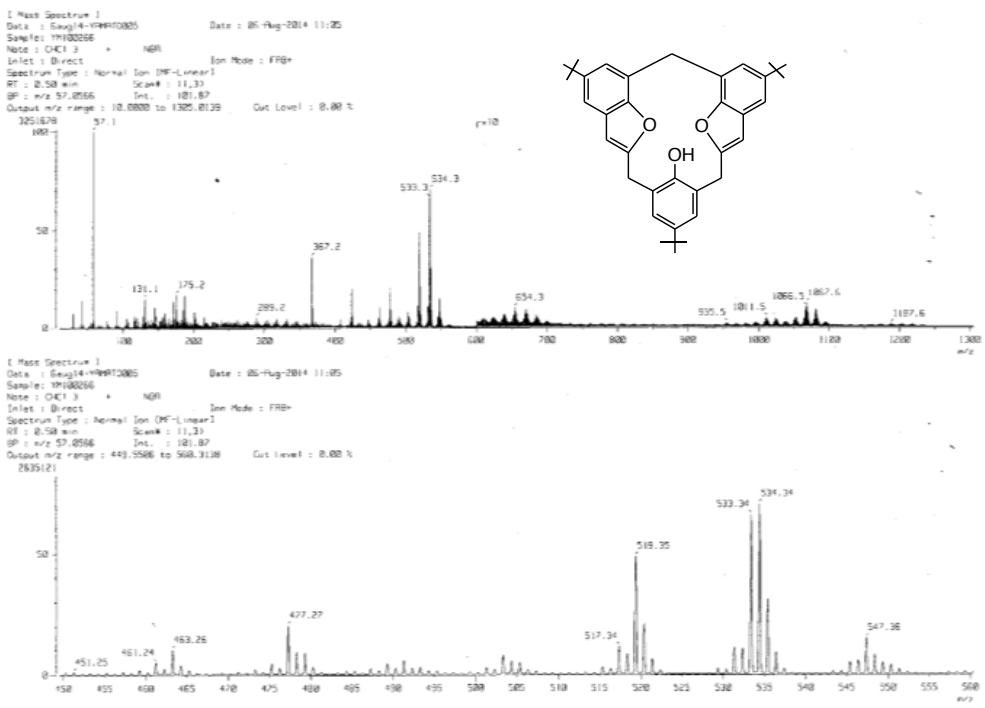

Figure S19: Mass spectrum of the compound **4a**.

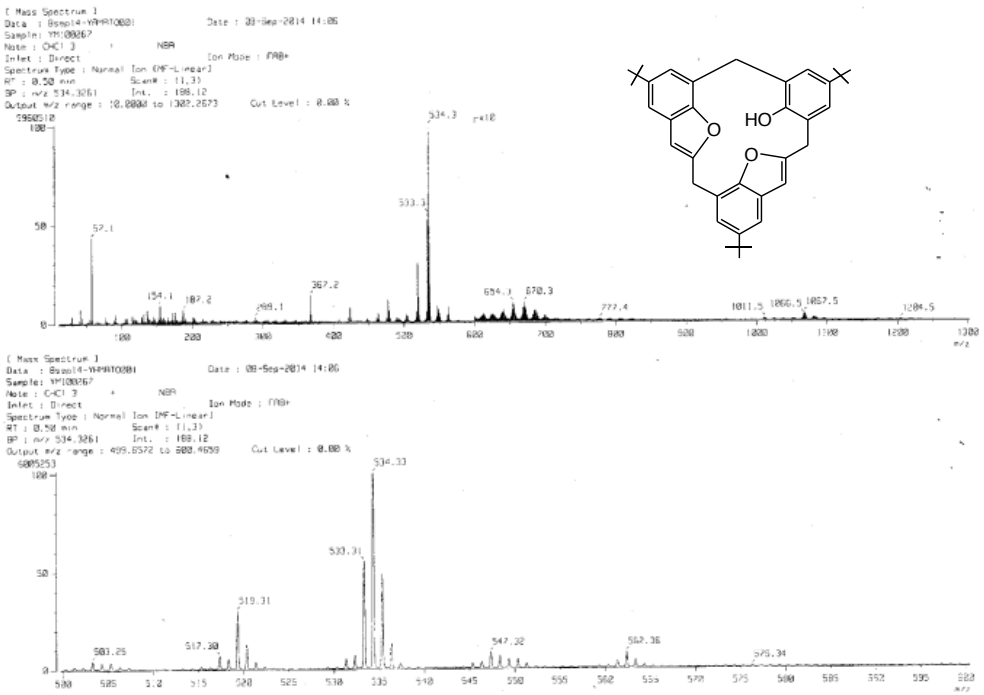

Figure S20: Mass spectrum of the compound **4b**.

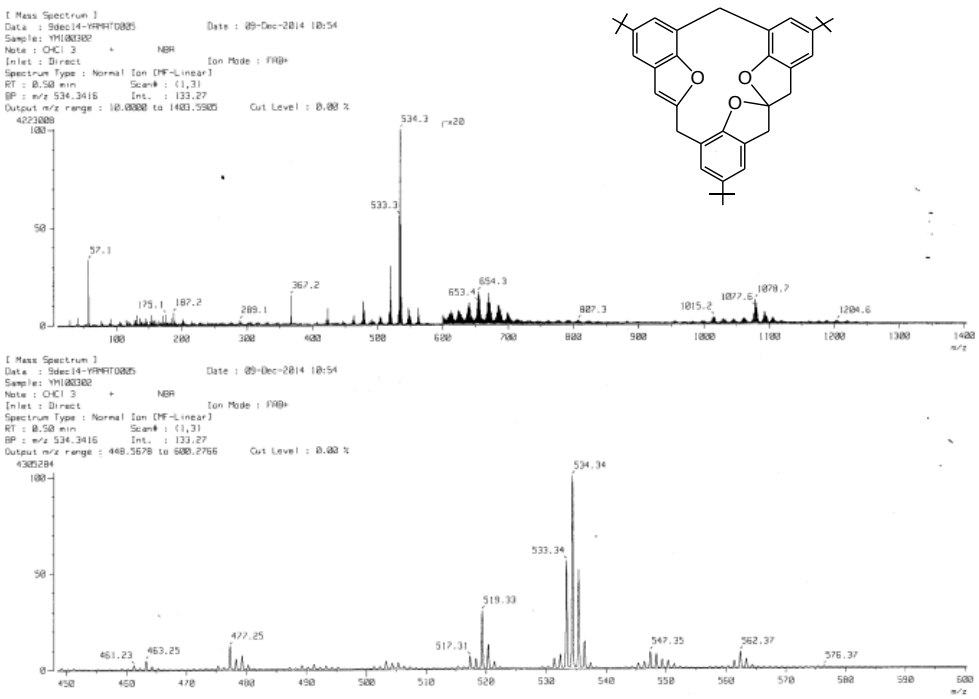

Figure S21: Mass spectrum of the compound **4c**.

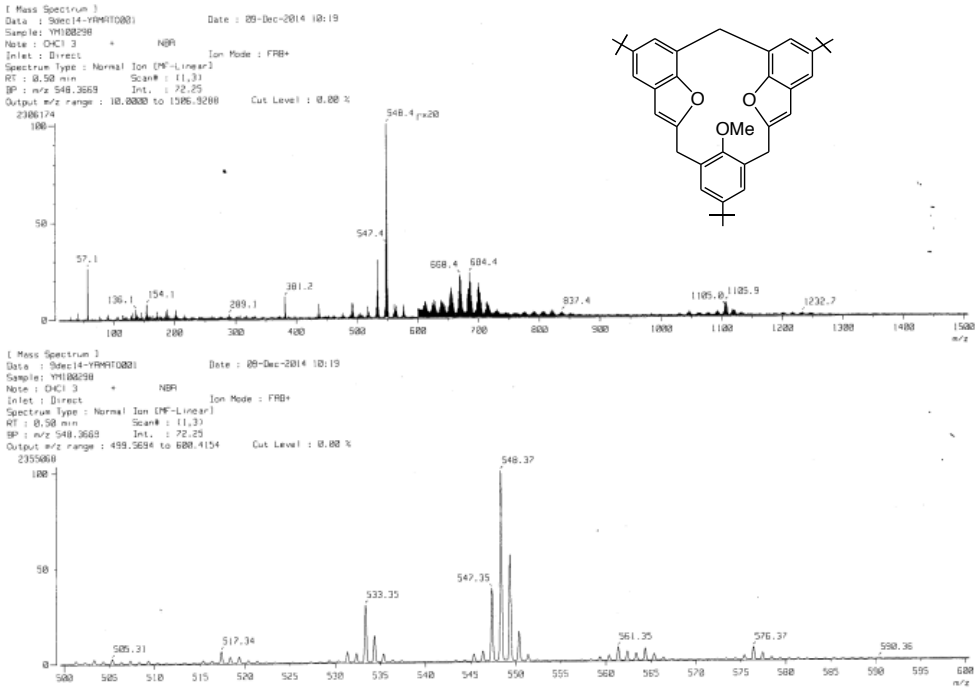

Figure S22: Mass spectrum of the compound **5a**.

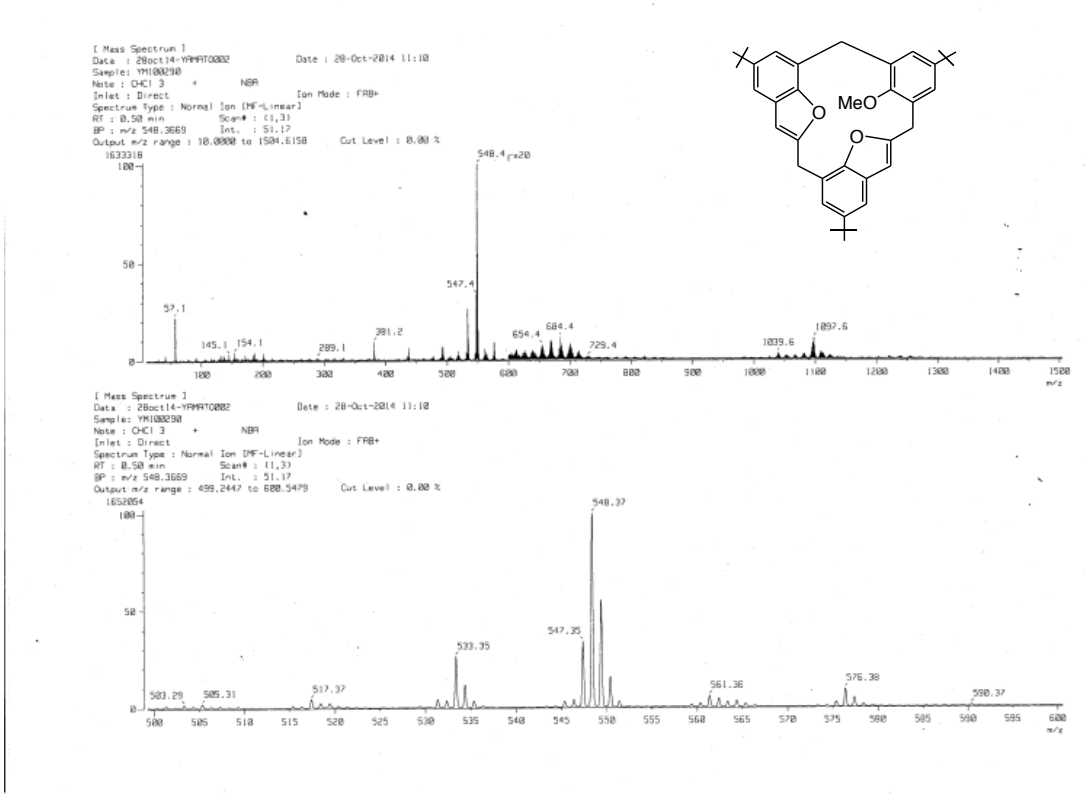

Figure S23: Mass spectrum of the compound **5b**.

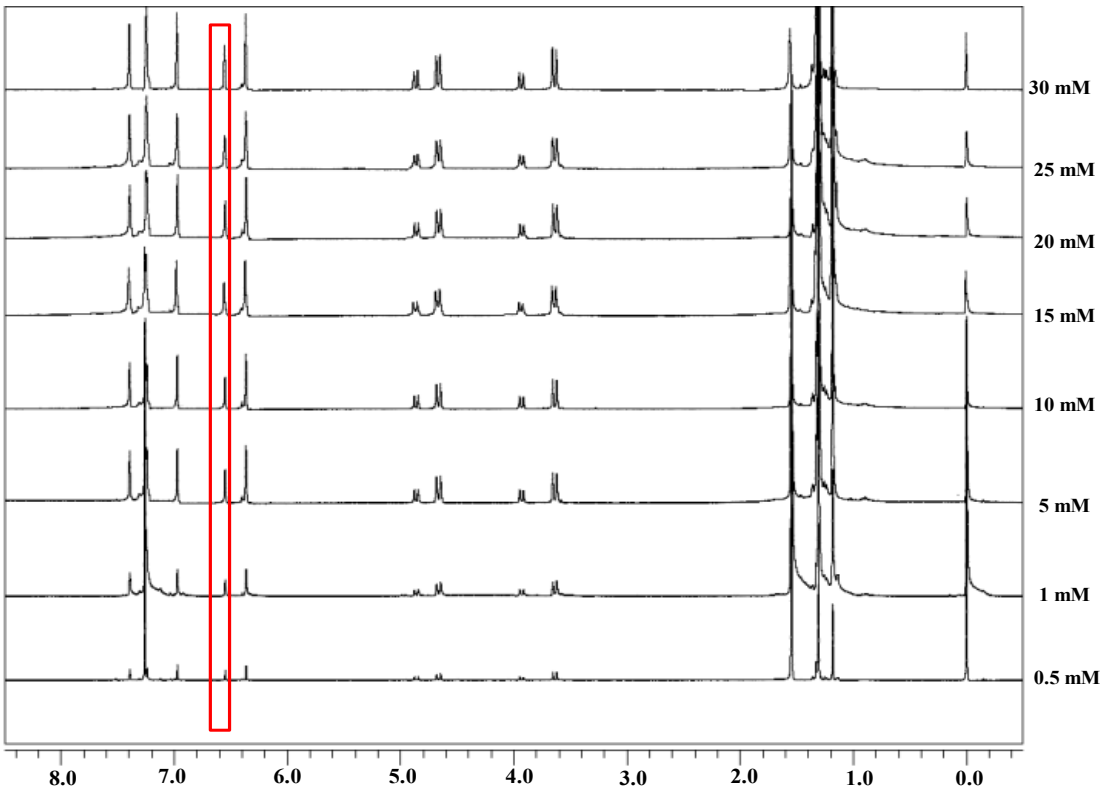

Figure S24: ^{1}H NMR Spectra of **4a** concentration studies 0.5 mM–30 mM (298 K, $CDCl_3$, 400 MHz).

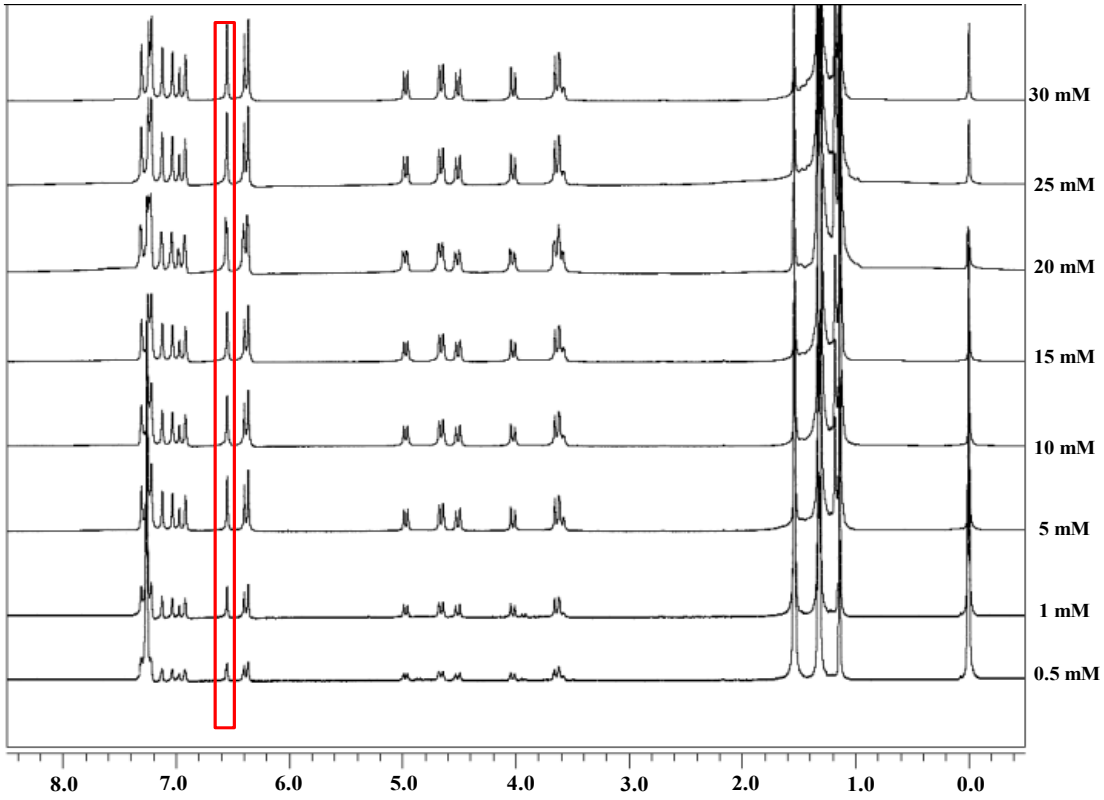

Figure S25: ^{1}H NMR Spectra of **4b** concentration studies 0.5 mM–30 mM (298 K, $CDCl_3$, 400 MHz).

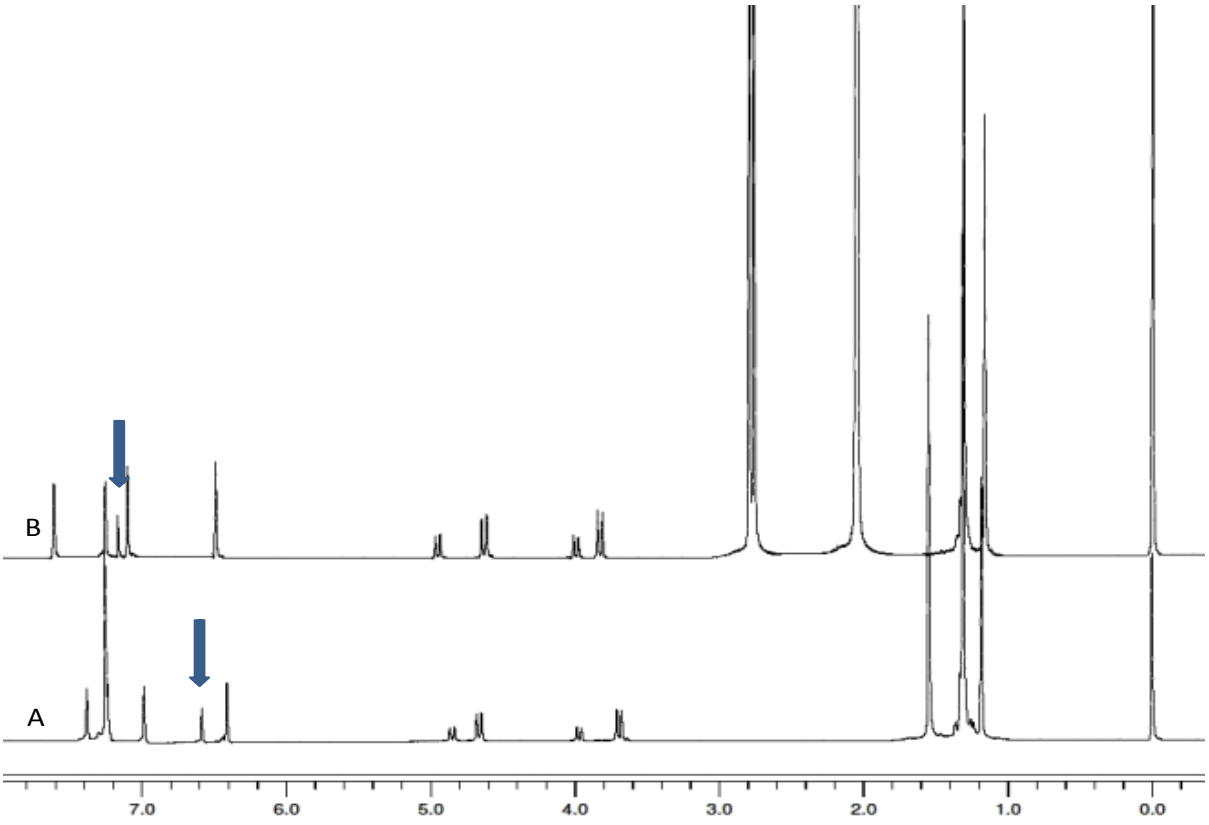

Figure S26: ^{1}H NMR spectra of **4a** (298 K, 5 mM; 400 MHz); (A) $CDCl_3$; (B) CD_3COCD_3.

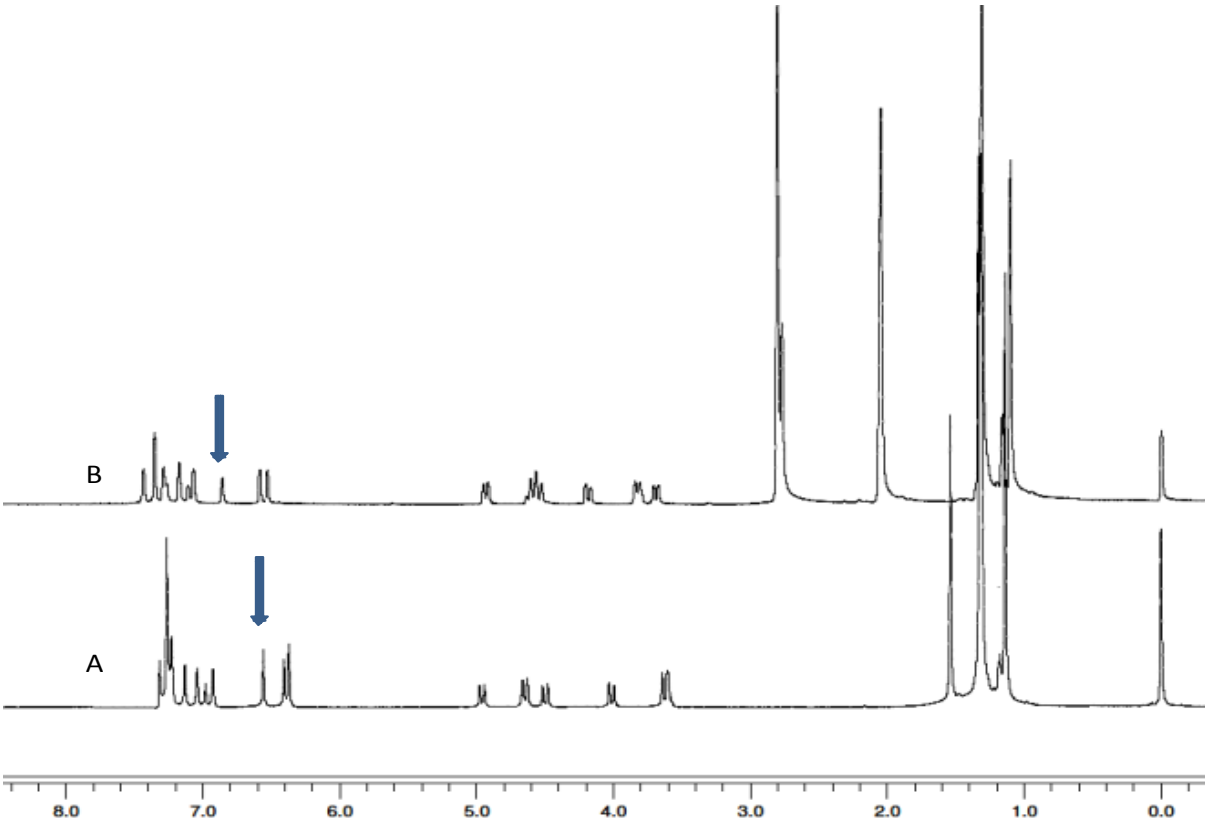

Figure S27: ^{1}H NMR spectra of **4b** (298 K, 5 mM; 400 MHz); (A) $CDCl_3$, (B) CD_3COCD_3.

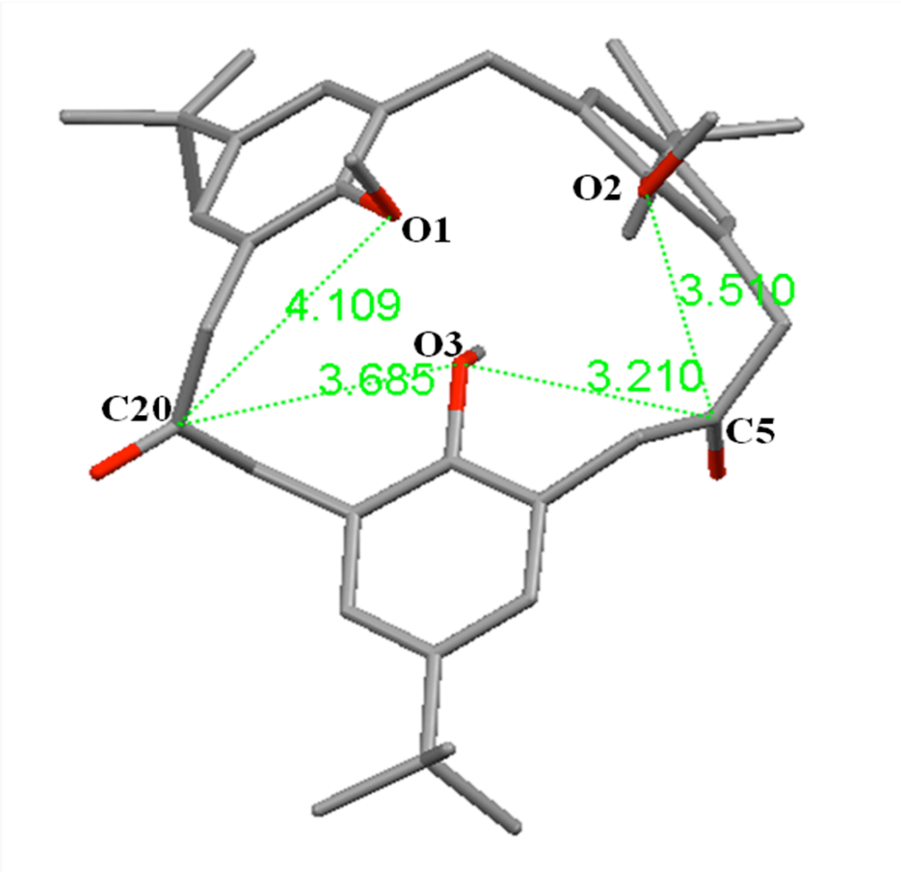

Figure S28: X-ray crystal structure of compound **3.**

X-ray crystallography

Table S1 **Summary of crystal data for 3, 4a and 5b**.[a,b]

Parameter	**3**	**4a**	**5b**
Empirical formula	$C_{40}H_{52}O_5$	$C_{37}H_{42}O_3$	$C_{38}H_{44}O_3$
Formula weight [g mol^{-1}]	612.43	534.71	548.76
Crystal system	monoclinic	orthorhombic	monoclinic
Space group	*P 2$_1$/c*	*Pcnn*	*C2/c*
A [Å]	12.237(3)	25.2718(5)	17.5245(3)
B [Å]	15.005(4)	13.4859 (3)	13.6997(3)
C [Å]	20.068(5)	17.4972 (4)	26.7366(5)
α [°]	90.0000	90.0000	90.0000
β [°]	101.798(18)	90.0000	104.033(7)
γ [°]	90.0000	90.0000	90.0000
Volume [Å^3]	3606.97	3343.9(3)	6227.3(3)
Z	4	8	8
Density, calcd [g m^{-3}]	1.106	1.191	1.171
Temperature [K]	123	123	123
Unique reflns	6548	5469	5695
Obsd reflns	4547	4089	4654
Parameters	418	362	370
R_{int}	0.0603	0.0417	0.0471
R[I>2σ(I)][a]	0.0769	0.0444	0.0629
wR[I>2σ(I)][b]	0.2516	0.1018	0.1639
GOF on F^2	1.097	1.016	1.041

[a] Conventional *R* on F_{hkl}: $\Sigma||F_o| - |F_c||/\sigma|F_o|$. [b] Weighted *R* on $|F_{hkl}|^2$: $\Sigma[w(F_o^2 - F_c^2)^2]/\Sigma[w(F_o^2)^2]^{1/2}$

General description for the computational study:

Density functional theory (DFT) computational studies were carried out to determine the geometry-optimized energies of compounds **4a**–**b** and **5a**–**b**.The starting structures were generated with the geometries based upon the X-ray structures of **4a** and **5b** and from the presumed structures of **4b** (derived from **4a**) and **5a** using SpartanPro'10 with the MMFF94 method.[1]The generated structures were then imported into Gaussian-09[2] and were geometry optimized in gas-phase with either the B3LYP or ωB97xD with 6-31G(d) basis set. The calculated energies (kJ mole^{-1}) for compounds **4a**, **4b**, **5a** and **5b** are shown in Table 2.As can be seen in Figure S30(4a), for compound **4a**the O1---H3 distance is 2.026 Å, which is shorter than that for the O2---H3 (2.460 Å) distance and is very close to the distance (2.182 Å) calculated from the single crystal X-ray analysis.

The results presented in Table S2 show that **4b** and **5b** were energetically more-favoured (in the gas-phase) by 3.792 or 3.083 and 89.974 or 74.718 kJ mole^{-1} than the corresponding structures of **4a** and **5a**, using B3LYP/6-31G(d) or ωB97xD/6-31G(d), respectively. As well, it can be noted that the *exo*-situated methoxy groups in **5a** and **5b** are energetically more-favoured than their corresponding *endo*-methoxy structures by 4.650 and 7.951 kJ mole^{-1}, respectively.

Table S2 DFT optimized energies of the synthesized MCPs.

Compound	**B3LYP** kJ mole^{-1}	**Δ**E（kJ mole^{-1}）	**ωB97xD** kJ mole^{-1}	**Δ**E（kJ mole^{-1}）
4a	-4360788.8	$\Delta E_{(4b-4a)}$ =-3.792	-4359514.4	$\Delta E_{(4b-4a)}$ =-3.083
4b	-4360792.6		-4359517.5	
5a(*exo*)	-4463872.2	$\Delta E_{(5b-5a)}$ =-89.974	-4462581.9	$\Delta E_{(5b-5a)}$ =-74.718
5b(*exo*)	-4463962.2		-4462656.6	
5a(*endo*)	-4463857.3	$\Delta E_{(5a exo-5a endo)}$= -14.897	-4462577.2	$\Delta E_{(5a exo-5a endo)}$= -4.650
5b(*endo*)	-4463947.5	$\Delta E_{(5b exo-5b endo)}$= -14.685	-4462648.6	$\Delta E_{(5b exo-5b endo)}$= -7.951

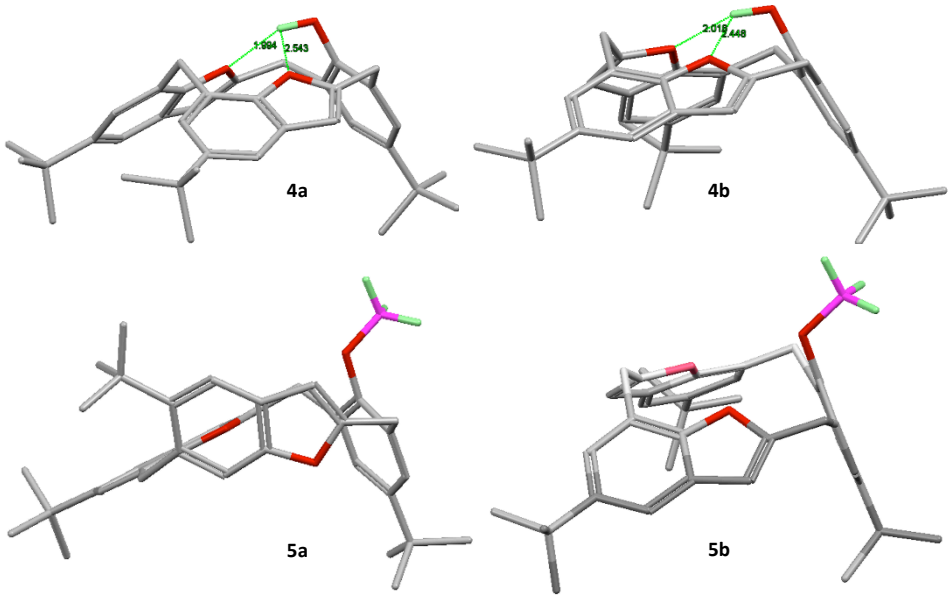

Figure S29. Geometry-optimized (B3LYP/6-31G(d)) structures of **4a**–**b** and **5a**–**b** (Ellipsoid): *Top Left*: **4a**; *Top Right*: **4b**; *Bottom Left*: 5a*partial cone*; and *Bottom Right*: **5b**. Colour code: hydrogen = white, carbon = dark grey, oxygen atom = red, except phenolic hydrogen and methoxy hydrogen = light green and methoxy carbon = magenta. All hydrogens except those phenolic hydrogen and methoxy hydrogen (light green) are omitted for clarity.

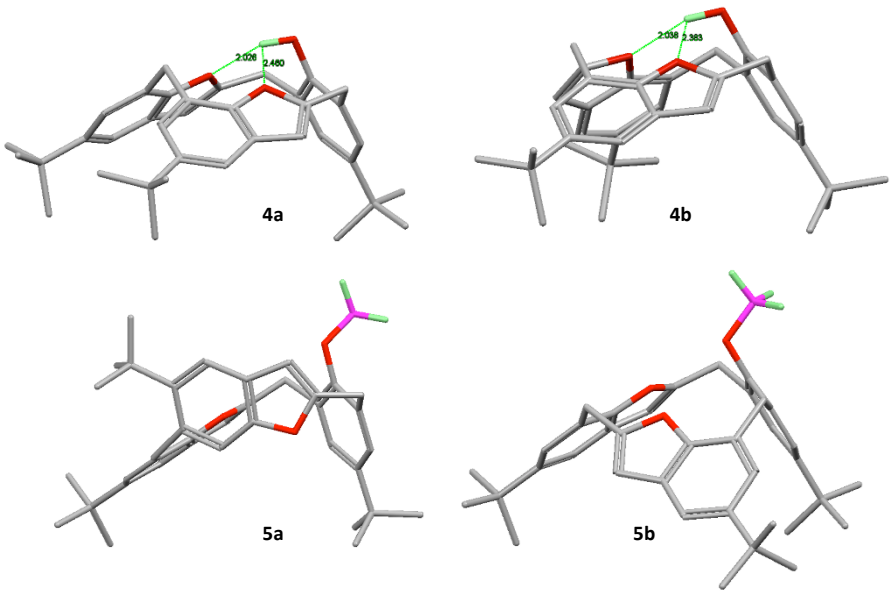

Figure S30. Geometry-optimized (ωB97xD/6-31G(d)) structures of **4a**–**b** and **5a**–**b** (Ellipsoid): *Top Left*: **4a**; *Top Right*: **4b**; *Bottom Left*: 5a*partial cone*; and *Bottom Right*: **5b**. Colour code: hydrogen = white, carbon = dark grey, oxygen atom = red, except phenolic hydrogen and methoxy hydrogen = light green and methoxy carbon = magenta. All hydrogens except those phenolic hydrogen and methoxy hydrogen (light green) are omitted for clarity.

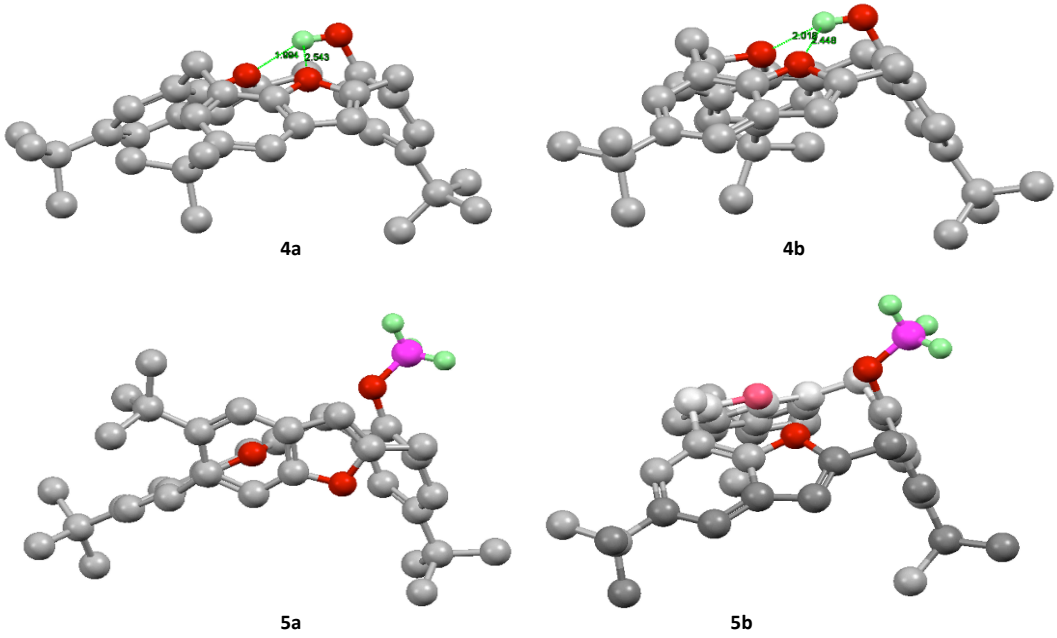

Figure S31. Geometry-optimized (B3LYP/6-31G(d)) structures of **4a**–**b** and **5a**–**b** (Ball-and-stick): *Top Left*: **4a**; *Top Right*: **4b**; *Bottom Left*: 5a*partial cone*; and *Bottom Right*: **5b**. Colour code: hydrogen = white, carbon = dark grey, oxygen atom = red, except phenolic hydrogen and methoxy hydrogen = light green and methoxy carbon = magenta. All hydrogens except those phenolic hydrogen and methoxy hydrogen (light green) are omitted for clarity.

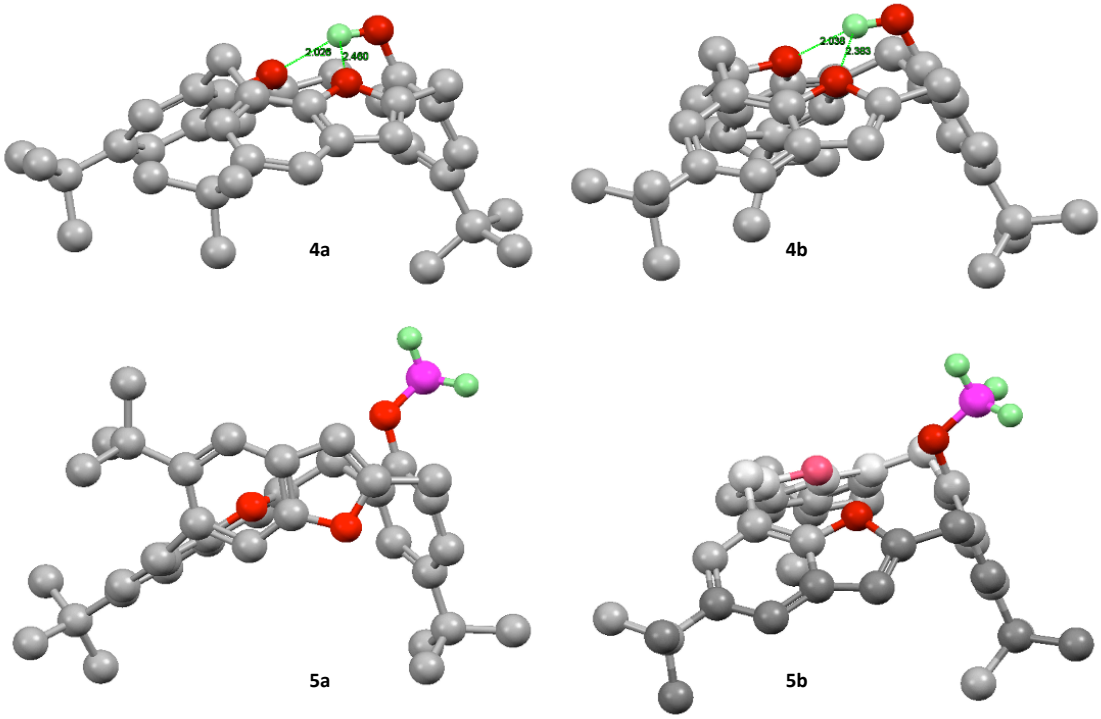

FigureS32. Geometry-optimized (ωB97xD/6-31G(d)) structures of **4a**–**b** and **5a**–**b**(Ball-and-stick): *Top Left*: **4a**; *Top Right*: **4b**; *Bottom Left*: 5a *partial cone*; and *Bottom Right*: **5b**. Colour code: hydrogen = white, carbon = dark grey, oxygen atom = red, except phenolic hydrogen and methoxy hydrogen = light green and methoxy carbon = magenta. All hydrogens except those phenolic hydrogen and methoxy hydrogen (light green) are omitted for clarity.

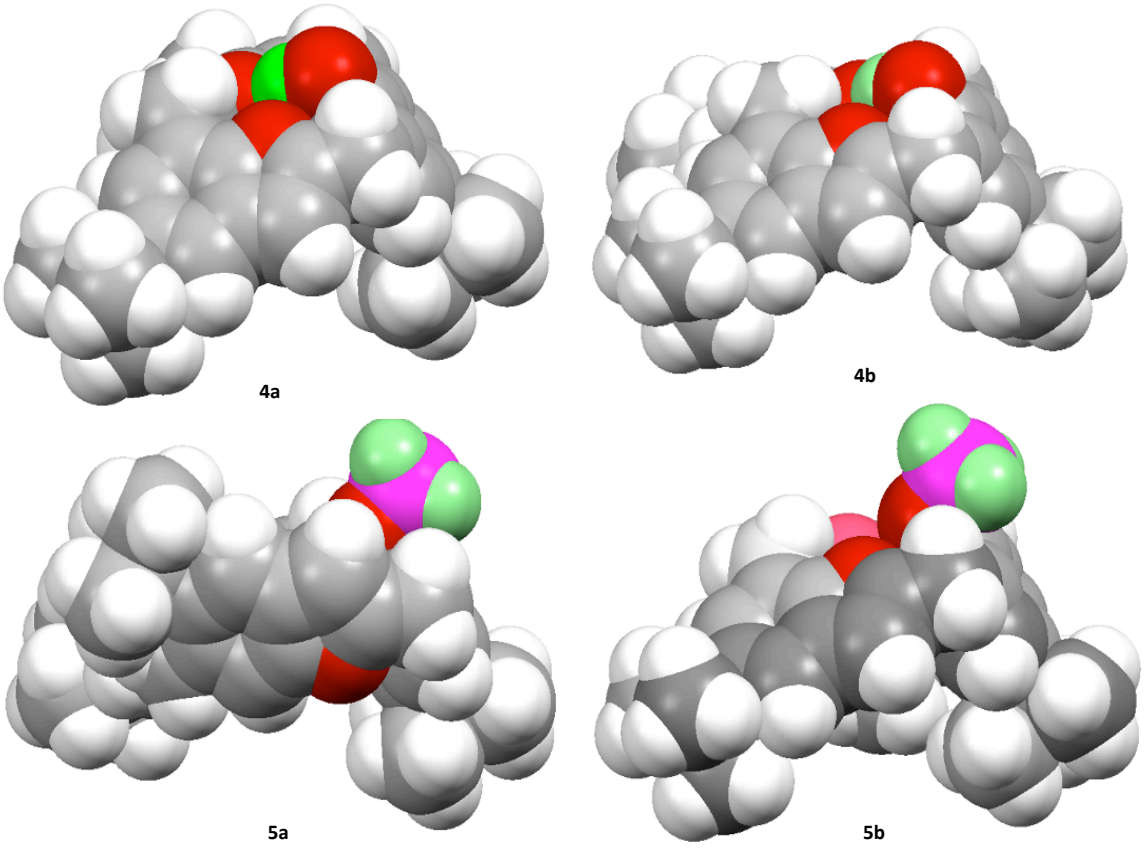

Figure S33. Geometry-optimized (B3LYP/6-31G(d)) structures of **4a**–**b** and **5a**–**b** (Spacefill): *Top Left*: **4a**; *Top Right*: **4b**; *Bottom Left*: **5a** *partial cone*; and *Bottom Right*: **5b**. Colour code: hydrogen = white, carbon = dark grey, oxygen atom = red, except phenolic hydrogen and methoxy hydrogen = light green and methoxy carbon = magenta. All hydrogens except those phenolic hydrogen and methoxy hydrogen (light green) are omitted for clarity.

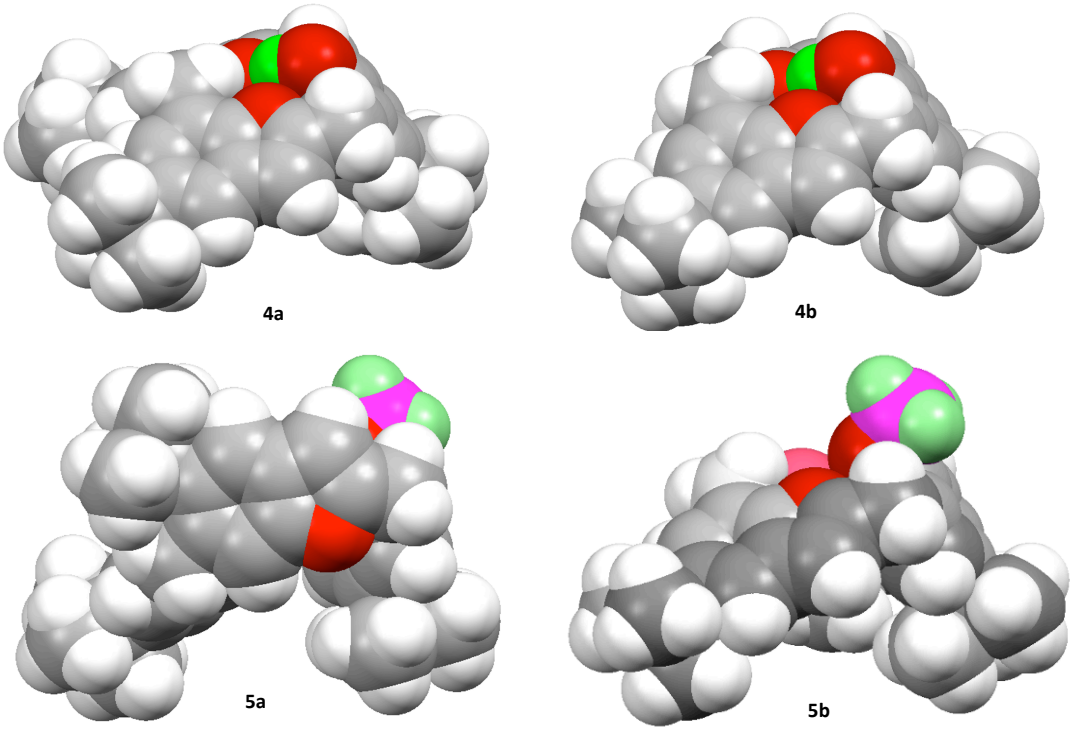

Figure S34. Geometry-optimized (ωB97xD/6-31G(d)) structures of **4a**–**b** and **5a**–**b** (Spacefill): *Top Left*: **4a**; *Top Right*: **4b**; *Bottom Left*: **5a***partial cone*; and *Bottom Right*: **5b**. Colour code: hydrogen = white, carbon = dark grey, oxygen atom = red, except phenolic hydrogen and methoxy hydrogen = light green and methoxy carbon = magenta. All hydrogens except those phenolic hydrogen and methoxy hydrogen (light green) are omitted for clarity.

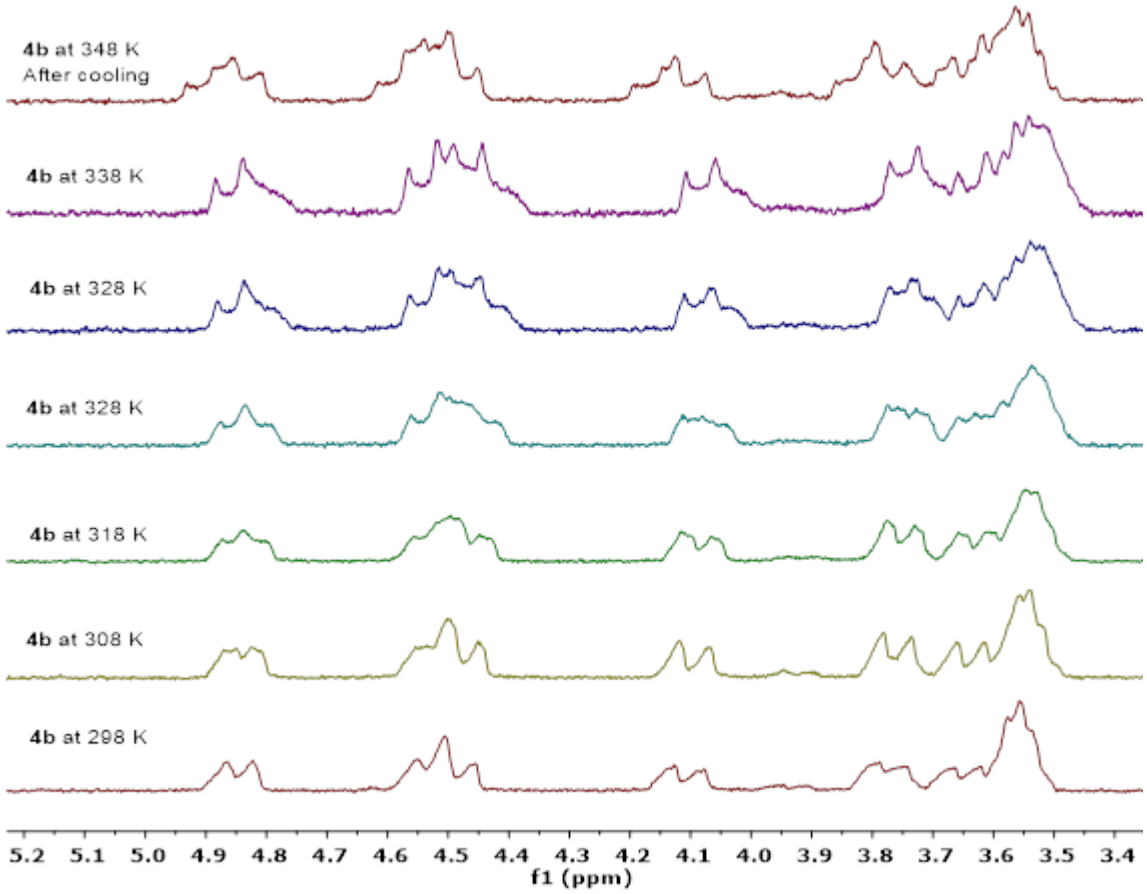

Figure S35: Partial VT-^{1}H NMR (300 MHz; 9:1 (v/v) CD_3CN:CD_2Cl_2) for compound **4b** at temperature 298 K to 348 K.

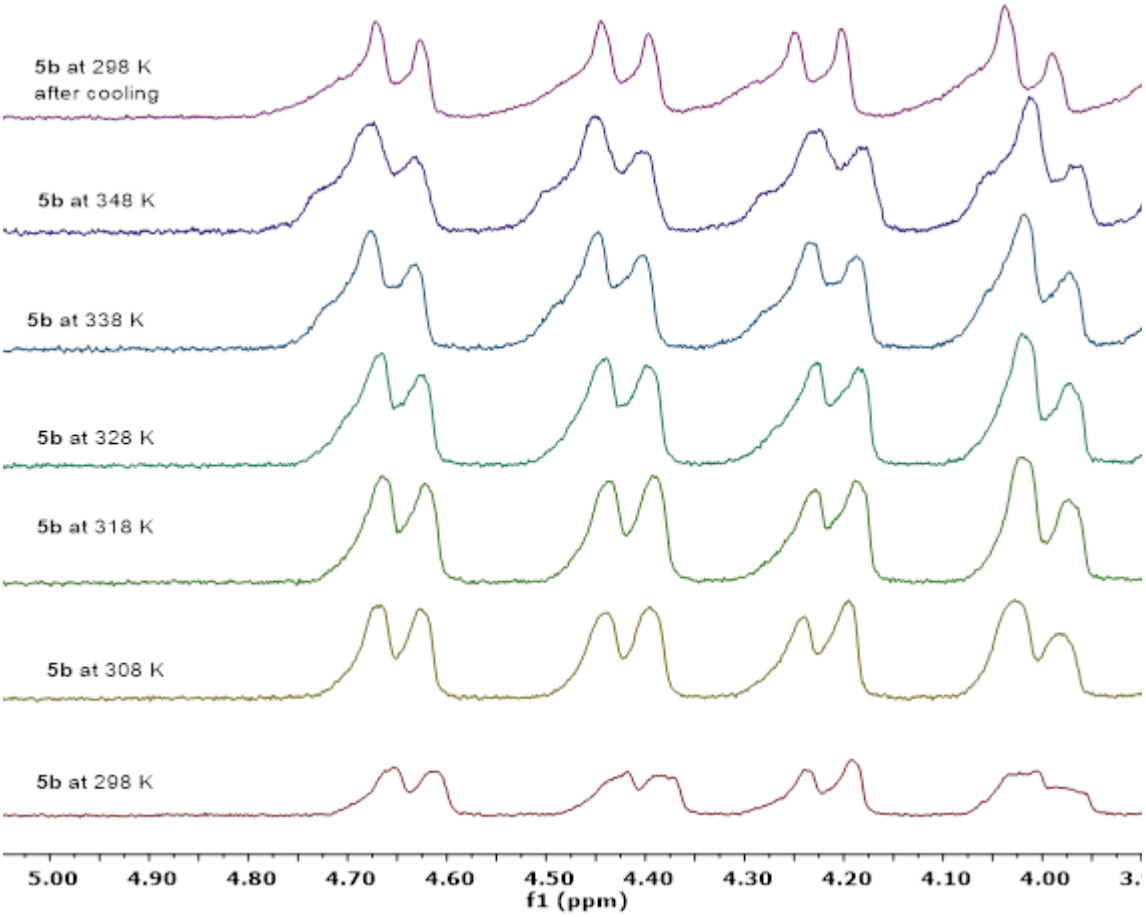

Figure S36: Partial VT-^{1}H NMR (300 MHz; 9:1 (v/v) CD_3CN:CD_2Cl_2) for compound **5b** at temperature 298 K to 358 K.

References

1. Initial molecular modeling calculations using the MMFF94 were performed using the *PC Spartan'10* software from Wavefunction Inc., Irvine CA.M.
2. Frisch, M. J.; Trucks, G. W.; Schlegel, H. B.; Scuseria, G. E.; Robb, M. A.; Cheeseman, J. R.; Scalmani, G.; Barone, V.; Mennucci, B.; Petersson, G. A.; Nakatsuji, H.; Caricato, M.; Li, X.; Hratchian, H. P.; Izmaylov, A. F.; Bloino, J.; Zheng, G.; Sonnenberg, J. L.; Hada, M.; Ehara, M.; Toyota, K.; Fukuda, R.; Hasegawa, J.; Ishida, M.; Nakajima, T.; Honda, Y.; Kitao, O.; Nakai, H.; Vreven, T.; Montgomery, Jr. J. A.; Peralta, J. E.; Ogliaro, F.; Bearpark, M.; Heyd, J. J.; Brothers, E.; Kudin, K. N.; Staroverov, V. N.; Keith, T.; Kobayashi, R.; Normand, J.; Raghavachari, K.: Rendell, A.; Burant, J. C.; Iyengar, S. S.; Tomasi, J.; Cossi, M.; Rega, N.; Millam, J. M.; Klene, M.; Knox, J. E.; Cross, J. B.; Bakken, V.; Adamo, C.; Jaramillo, J.; Gomperts, R.; Stratmann, R. E.; Yazyev, O.; Austin, A. J.; Cammi, R.;

Pomelli, C.; Ochterski, J. W.; Martin, R. L.; Morokuma, K.; Zakrzewski, V. G.; Voth, G. A.; Salvador, P.; Dannenberg, J. J.; Dapprich, S.; Daniels, A. D.; Farkas, O.; Foresman, J. B.; Ortiz, J. V.; Cioslowski, J.; Fox, D. J. *Gaussian 09, Revision D.01*; Gaussian, Inc., Wallingford CT, 2013.